

THE IDENTIFICATION OF PROBABLE SiS EMISSION AT 13–14 μm IN SPECTRA OF GALACTIC S STARS

G. C. SLOAN¹, S. HONY², K. SMOLDERS³, L. DECIN³, A. A. ZIJLSTRA⁴, M. W. FEAST^{5,6}, F. VAN WYK⁶, J. TH. VAN LOON⁷,
M. A. T. GROENEWEGEN⁸, AND R. SAHAI⁹

¹ Astronomy Department, Cornell University, Ithaca, NY 14853-6801, USA; sloan@isc.astro.cornell.edu, jbs@isc.astro.cornell.edu, jrh13@cornell.edu

² Laboratoire AIM, CEA/DSM-CNRS, University Paris Diderot, DAPNIA/SAP, 91191 Gif-sur-Yvette, France; sacha.hony@cea.fr

³ Department of Physics and Astronomy, Institute for Astronomy, K. U. Leuven, Celestijnenlaan 200B, 3001 Leuven, Belgium; kristof.smolders@ster.kuleuven.be,
leen.decin@ster.kuleuven.be

⁴ School of Physics & Astronomy, University of Manchester, P.O. Box 88, Manchester M60 1QD, UK; albert.zijlstra@manchester.ac.uk

⁵ Astrophysics, Cosmology and Gravitation Centre, and Astronomy Department, University of Cape Town, Rondebosch 7701, South Africa

⁶ South African Astronomical Observatory, P.O. Box 9, Observatory, 7935, South Africa; mwf@ast.uct.ac.za, fvw@sao.ac.za

⁷ Astrophysics Group, Lennard-Jones Laboratories, Keele University, Staffordshire ST5 5BG, UK; jacco@astro.keele.ac.uk

⁸ Royal Observatory of Belgium, Ringlaan 3, B-1180 Brussels, Belgium; marting@oma.be

⁹ Jet Propulsion Laboratory, MS 183-900, California Institute of Technology, Pasadena, CA 91109, USA; sahai@jpl.nasa.gov

Received 2010 June 18; accepted 2011 January 12; published 2011 February 16

ABSTRACT

A sample of 90 Galactic S stars observed by the *Spitzer Space Telescope* includes two sources with unusual low-contrast spectral structure between 7 and 14 μm . The most likely estimate of the spectral continuum leads to the identification of molecular emission features from SiS at 7 and 13–14 μm . The spectra also show what is best described as featureless excess emission, most likely from iron dust but possibly from amorphous carbon, as well as an emission feature from amorphous alumina dust peaking at 11–12 μm . The spectra show long-wavelength excesses from cool dust grains in an extended envelope and additional emission features of unknown origin.

Key words: circumstellar matter – infrared: stars – stars: AGB and post-AGB – stars: mass-loss

1. INTRODUCTION

Merrill (1922) first identified S stars, which show absorption bands from ZrO in their optical spectra (Merrill 1923), along with bands from other unusual oxides such as LaO (Keenan 1948) and YO (e.g., Keenan 1966). S stars differ from oxygen-rich M giants, where TiO bands dominate the optical spectra, and carbon stars, with CN-dominated spectra. These chemical differences result from the dredge-up of carbon and other fusion products while stars evolve on the asymptotic giant branch (AGB; e.g., Iben & Renzini 1983). With enough dredge-ups, an M giant becomes a carbon star. Fujita (1939, 1940) proposed that M giants, S stars, and carbon stars could be distinguished by the relative abundances of C, N, and O, but it would be another decade before it was recognized that S stars had C/O ratios near unity and that N was unimportant (Bidelman 1950).

The CO molecule will form in stellar outflows until it exhausts either C or O, leaving only the other free to produce dust (see the review by Habing 1996, and references therein). In S stars, nearly all of the C and O will be exhausted, which will lead to unusual chemistry in the outflows. Sloan & Price (1998) found that S and MS stars observed by the Low-Resolution Spectrometer on the *Infrared Astronomical Satellite (IRAS)* produced dust shells which were dominated by alumina dust instead of silicates, and they suggested that the alumina, which will form first, had exhausted the available oxygen.

To investigate the consequences of this unusual chemistry, S. Hony designed a program (Program 30737) to observe 90 S stars with the Infrared Spectrograph (IRS; Houck et al. 2004) on the *Spitzer Space Telescope* (Werner et al. 2004). A full examination of this sample is in preparation. The sample includes 53 stars which are naked or nearly dust-free and 35 showing dust emission features in their spectra,¹⁰ along with two

sources showing an unusual spectral emission feature peaking at 13–14 μm not observed prior to the *Spitzer* mission.

This paper concentrates on these two objects, describing how the spectra were obtained and reduced in Section 2, and in Section 3, presenting additional photometry, tackling the difficult question of estimating the stellar continuum in the spectra, and describing the consequences. The best estimate of stellar continuum requires an additional featureless spectral component, which may be iron dust. This scenario leads to the identification of emission features at 7 and 13–14 μm , which we identify as emission from molecular SiS. In Section 4 we discuss the context.

2. OBSERVATIONS AND DATA REDUCTION

The spectra were observed with the IRS in its standard low-resolution staring mode, which places the star in two nod positions, first in the two Short-Low (SL) apertures and then in the two Long-Low (LL) apertures. The resulting spectrum runs from 5 to 37 μm with an average resolution ($\lambda/\Delta\lambda$) of ~ 100 .

We started with flat-fielded images from the S18.7 pipeline release from the Spitzer Science Center (SSC). Before extraction, we removed the background emission by differencing images in the opposite aperture in SL and in the opposite nod in LL. We also cleaned the images using the imclean IDL package¹¹ to replace pixels flagged as bad or as rogue pixels.

We extracted spectra from the differenced and cleaned images using pipeline modules available with the SSC's *Spitzer* IRS Custom Extractor (SPICE). To calibrate the spectra, we generated spectral corrections using the K0 giant HR 6348. We eliminated discontinuities between the orders by multiplying each segment by a scalar correction. These discontinuities arise primarily from pointing errors, so we normalized the segments up to what is presumably the best-centered segment, which in

¹⁰ These numbers may change with further analysis.

¹¹ Available from the SSC within the irs-clean package.

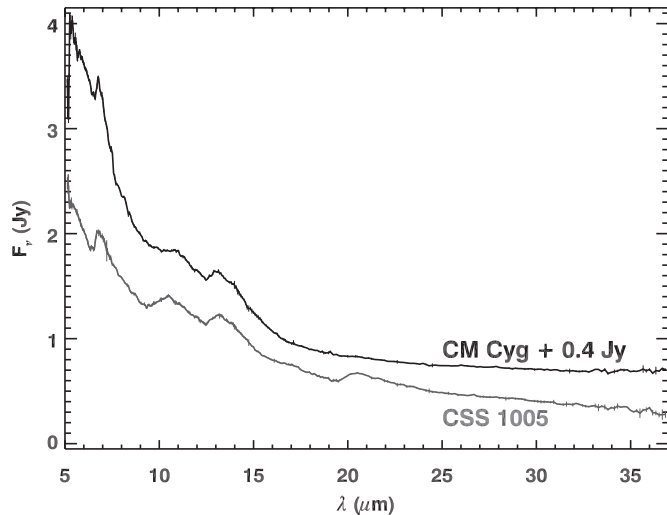


Figure 1. IRS spectra of CM Cyg (top) and CSS 1005 (bottom). CM Cyg has been shifted up 0.4 Jy so the spectra do not overlap.

both cases was LL order 2 (14–21 μm). The correction to SL for CM Cyg was unusually large, 35%, but the difference between the spectra from the individual nod positions is consistent with partial truncation of the source by the slit due to a slight mispointing. As discussed below, the corrected spectrum agrees with photometric measurements. For CSS 1005, the corrections to SL were $\sim 10\%$, which is more typical. The final step was to trim poor data from the ends of the segments.

3. ANALYSIS

Figure 1 presents the IRS spectra of CM Cyg and CSS 1005. Both have emission peaks at 7, 11, and 13–14 μm . One source in another published sample also shows a similar 13–14 μm emission feature, the star BFM 1 in the Small Magellanic Cloud (SMC; Sloan et al. 2008), which is also an S star. BFM 1 received an infrared spectral classification of 2.ST (extending the classification system of Kraemer et al. 2002), and in that scheme, both of these spectra are 2.ST as well.

The location of the stellar continuum in the spectra of CM Cyg and CSS 1005 is not obvious. If, for example, the 6–8 μm region defines the continuum, then the observed spectral structure results from emission features, but if the continuum passes through the spectra at 13–14 μm , then all of the features appear in absorption.

Relatively little is known about CSS 1005, except that it is an S star (Stephenson 1984). CM Cyg is better studied. It has a spectral class of S4/6.5e (Keenan & Boeshaar 1980), which implies a C/O ratio of ~ 0.98 –0.99. Ake (1979) classified two spectra of CM Cyg as S4e and SC2. It is a Mira variable with a period of 254.43 days (Templeton et al. 2005). AAVSO data reveal a steady pulsation period and a visual amplitude of 4.7 mag. The most recent visual maximum in those data came on JD 2544031.5.

3.1. The Continuum of CM Cyg

While we do not have near-infrared photometry contemporary with the IRS observation, the steady pulsational properties of CM Cyg make it possible to use the Two Micron All Sky Survey (2MASS) photometry (Skrutskie et al. 2006) to constrain the continuum in the IRS data. We have dereddened the data using an estimated A_v of 0.54, based on the extinction maps of Schlegel

Table 1
Near-infrared Photometry

JD	J	H	K or K_s	L	Notes
CM Cyg					
2451695	6.39	5.45	5.01	...	2MASS
2451695	6.24	5.36	4.93	...	Dereddened 2MASS
2454027	5.98	5.08	4.69	...	Phase-corrected 2MASS
CSS 1005					
2451291	7.65	6.19	5.48	...	2MASS
2451291	7.03	5.81	5.23	...	Dereddened 2MASS
2454025	Date of IRS observation
2454232	6.26	5.05	4.63	4.14	SAAO
2454232	5.60	4.62	4.39	3.99	Dereddened SAAO
2454539	6.60	5.55	5.12	4.62	SAAO
2454539	5.94	5.11	4.88	4.47	Dereddened SAAO

et al. (1998)¹² and the extinction curves of Rieke & Lebofsky (1985), shifted to account for the central wavelengths of the 2MASS filters. Our estimates of the reddening are smaller than those of Yang et al. (2006). Based on the period– K relation of Whitelock et al. (2008), CM Cyg has a distance modulus of approximately 12.0, compared to 13.0 for the Outer or Cygnus Arm of the Galaxy (Negueruela & Marco 2008). Thus, the extinction maps are likely to include the effect of some dust behind CM Cyg, but most of the reddening will be between the star and us.

It is also necessary to correct for the phase of variability and likely molecular band absorption in the near-infrared. The IRS observed CM Cyg at an optical phase of 0.98 (JD 2452047), while 2MASS observed it at a phase of 0.82 (JD 2451695). Photometric data presented by Smith et al. (2006) reveal a typical optical-to-infrared phase lag of 0.20 ± 0.06 for stars with comparable periods, which shifts the apparent infrared phases to 0.78 (IRS) and 0.62 (2MASS). From a sample of 12 Miras with periods between 200 and 300 days studied by Catchpole et al. (1979), we find typical amplitude ratios of $\Delta J/\Delta V = 0.12 \pm 0.3$, $\Delta H/\Delta V = 0.13 \pm 0.3$, and $\Delta K/\Delta V = 0.11 \pm 0.2$. Fitting a cosine function to the AAVSO data, correcting for phase difference, optical-to-infrared phase lag, and amplitude ratios, we reconstruct the phase-corrected photometry as given in Table 1. We estimate the uncertainties to be between 6% and 8%.

Figure 2 compares the IRS spectrum to derived photospheric fluxes at J , H , and K after correcting the 2MASS data for reddening, phase of variability, and molecular band absorption. This last correction is based on the recalibrated spectral template of β Gru (M5 III; Engelke et al. 2006). We fit this spectrum with a 3700 K Engelke function (Engelke 1992). Applying 2MASS filter functions reveals that the continuum is above the spectrum by 0.86 mag at J and 0.12 mag at H , while it passes through the spectrum at K_s . The correction at J is almost certainly too large for CM Cyg, since many of the oxides which affect the spectrum at these wavelengths will be missing in an almost pure S star. The impact of molecules is small at H and negligible at K , because the 2MASS K_s filter cuts off below 2.3 μm , avoiding almost all of the CO overtone band at 2.4 μm . Consequently, we will require that any estimate of the continuum pass through the photometry at K and not far from H .

A 3600 K Planck function fitted at K comes close to H , but falls well under the IRS spectrum. We believe that this is the

¹² Accessed via the interface maintained by the Infrared Science Archive (IRSA).

best estimate for the stellar temperature because it approximates the measured $H - K$ color. Raising the temperature would eliminate the error at H , but the shortfall past $5 \mu\text{m}$ would grow. Decreasing the temperature would improve the fit to the spectrum, but worsen the discrepancy at H .

Figure 2 also includes photometry from the *IRAS* Faint Source Catalog (Moshir et al. 1990) and the *Akari* all-sky survey (Ishihara et al. 2010). We have adjusted the *IRAS* data with color corrections for stellar spectra in the Explanatory Supplement (Beichman et al. 1988). These photometric data confirm that the mid-infrared emission in these stars shows an excess over what can be estimated from the near-infrared.

We have attempted to be conservative, assuming the highest reasonable reddening correction, which raises the near-infrared photometry. We have also used a Planck function, which does not fall to longer wavelengths as steeply as the semiempirical Engelke function or a model continuum including the effect of the H^- ion. Nevertheless, some source of relatively featureless excess is still required to account for the difference between the assumed photospheric continuum and the *IRS* spectrum.

Recent *Spitzer* photometric studies of AGB stars in globular clusters provide some guidance to this problem. Boyer et al. (2009) and McDonald et al. (2009) found low-contrast excesses in the mid-infrared which Boyer et al. suggested might be from amorphous carbon. Given the oxygen-rich nature of the AGB stars in their globular cluster samples, amorphous carbon is unlikely. McDonald et al. (2010), looking at *IRS* spectra of similar sources, proposed iron dust as a better explanation.

Figure 2 fits several simple dust models to the “continuum” of CM Cyg. Two are based on iron grains, using the dielectric constants determined by Ordal et al. (1988) and an assumed grain radius of $0.3 \mu\text{m}$. Fitting to the valleys of the spectrum, which as explained below we believe to be the most likely scenario, requires a dust temperature of 660 K, with an excess of 37% over the stellar photosphere at its peak near $10 \mu\text{m}$. Because iron at these temperatures emits negligibly in the near-infrared, we are free to add more iron to fit any part of the spectrum we identify as “continuum.” Figure 2 also includes a larger excess of iron at 450 K which passes through the spectrum at its peaks at 7 and 13–14 μm . In this scenario, the excess over the photosphere is 99% at $10 \mu\text{m}$.

While amorphous carbon is unlikely in O-rich AGB stars, CM Cyg is an S star with a C/O ratio only slightly less than unity. To consider the possibility that amorphous carbon could be present in our spectra, we use the optical constants by Zubko et al. (1996, ACAR). Figure 2 shows that amorphous carbon could fit any “continuum” about as well as iron. Fitting the lower “continuum” requires a dust temperature of 780 K and an excess of 37% over the continuum at $10 \mu\text{m}$, while the upper fit has $T = 470 \text{ K}$ and a 97% excess at $10 \mu\text{m}$.

For both iron and amorphous carbon dust, we assumed an optically thin emitting region, and for ease of calculation, spherical grains of uniform radius and temperature. We adjusted the temperature and amount of dust to fit the assumed continuum. If the lower continuum arises from iron dust, a total grain mass of $\sim 2 \times 10^{-9} M_{\odot}$ is required. Iron is unusual because the estimated dust mass is a strong function of grain size. For most dust species, the electrical component of the optical efficiency dominates, and because it scales with grain size a , to first order a cancels when determining the mass. But for iron, the magnetic component dominates, and it depends on a^3 , such that dust mass $\propto a^{-2}$. For this reason we have considered grains with $a = 0.3 \mu\text{m}$. Even larger Fe grains would require less mass, but

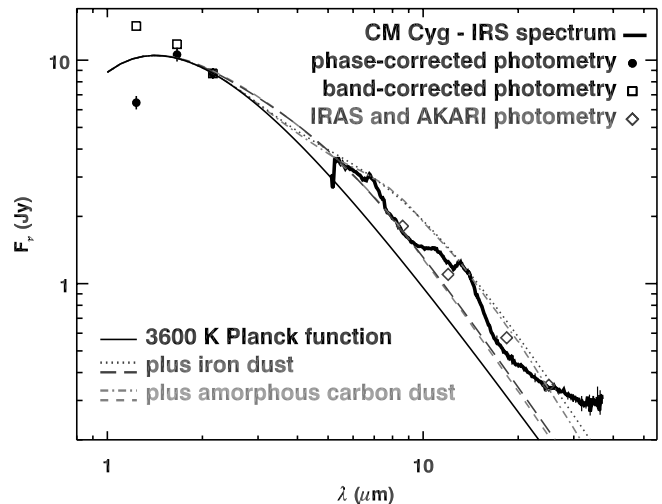


Figure 2. Fitting the continuum in CM Cyg. The dereddened and phase-corrected 2MASS photometry in Table 1 is plotted with filled circles. The open boxes include corrections for molecular bands, but these corrections are likely too large for a pure S star like CM Cyg. A 3600 K Planck function fitted through the K band lies well under the *IRS* spectrum. The open diamonds show that the photometry from *Akari* (8.6 and 18.4 μm) and *IRAS* (12 and 25 μm) presents a similar problem. A pseudo-continuum from either iron dust or amorphous carbon dust can make up the difference, but these dust species can be fit through either the valleys or peaks in the spectrum (curves with dots and dashed curves, respectively). Thus, the *JHK* photometry poorly constrains the continuum in the *IRS* data.

because the sizes involved invalidate the dipole approximation at these wavelengths ($a/\lambda \lesssim 0.1$), more sophisticated modeling is required.

To assess whether the derived iron dust mass is reasonable, we need to estimate the distance of the dust from the star and make some assumptions. If we assume a mass-loss rate of $10^{-7} M_{\odot} \text{ yr}^{-1}$, solar abundances, and that all of the iron condenses into dust, then the dust mass would correspond to about nine years of mass loss. We can estimate the distance from the star to the iron grains using Planck mean opacities, but this method is complicated by the fact that the optical constants of iron are measured only for $\lambda > 0.67 \mu\text{m}$. For $0.3 \mu\text{m}$ iron grains, we obtain a distance of $\sim 60 R_{*}$, but this is certainly an underestimate. Amorphous carbon and iron have roughly similar optical properties, and substituting with amorphous carbon constants, the distance is $\sim 90 R_{*}$. If we further assume an outflow velocity of 10 km s^{-1} and $R_{*} \sim 1 \text{ AU}$, the grains are moving at $\sim 2 R_{*} \text{ yr}^{-1}$. At these distances, nine years of mass loss would produce a range of 70 K in temperature, which is not unreasonable. The amount of iron could be reduced to even more reasonable amounts if the grains were larger, or possibly if they were non-spherical or if the mass loss were episodic.

Amorphous carbon is a more normally behaved grain material, and the dust mass does not depend strongly on grain size. However, for $a > 0.1 \mu\text{m}$, the grains emit strongly enough at K that their contribution becomes non-negligible. We consequently set $a = 0.1 \mu\text{m}$. Fitting the lower continuum requires $1.4 \times 10^{-9} M_{\odot}$ of amorphous carbon. Again assuming solar abundances and a mass-loss rate of $10^{-7} M_{\odot} \text{ yr}^{-1}$, if all of the carbon were tied up in dust, then the observed carbon could be produced in only 3.5 years. Unfortunately, the formation of CO in the outflows will consume most of the available carbon, leaving perhaps only 10% of the C for the dust. In that case, the amorphous carbon in the spectrum would account for 35 years

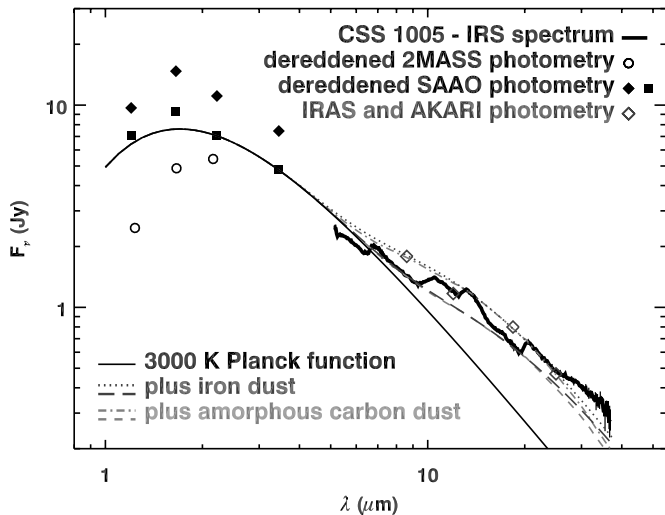


Figure 3. Fitting the continuum in CSS 1005. The photometry are dereddened, but have had no further corrections. Otherwise, the symbols and curves are as in Figure 2. As with CM Cyg, the possible presence of iron dust or amorphous carbon dust allows many possible fits of a pseudo-continuum to the data.

of mass loss. At 780 K, the grains are $\sim 34 R_*$ from the central star, but in 35 years, the grains would move $\sim 70 R_*$.

Iron dust appears to be the more plausible option. If we consider that CM Cyg has slightly more oxygen than carbon, the expected formation of CO strengthens the case for iron. Attempting to fit the upper “continuum” requires a dust mass which is implausible for either iron or amorphous carbon. Furthermore, if the maximum spectral features define the continuum, then CM Cyg would be embedded in a circumstellar envelope producing deep absorption bands from 7 to $10 \mu\text{m}$ and from 14 to $26 \mu\text{m}$. No such absorbers are known. On the other hand, if the smaller excess passing through the spectral minimum at $7.5\text{--}9.5 \mu\text{m}$ is correct, then the spectrum has additional emission features at ~ 7 , $\sim 11\text{--}12$, and $\sim 13\text{--}14 \mu\text{m}$. As Sections 3.3 and 3.4 show below, we can explain these remaining features as a combination of amorphous alumina dust emission and molecular SiS emission bands.

3.2. The Continuum of CSS 1005

Out of the 90 S stars observed in *Spitzer* Program 30737, only CSS 1005 presents a spectrum similar to CM Cyg. While we have 2MASS photometry for both sources, the lack of light-curve information for CSS 1005 prevents phase corrections. However, we have obtained additional photometry at the 0.75 m telescope at the South African Astronomical Observatory (SAAO; see Table 1). The extinction maps of Schlegel et al. (1998) suggest a maximum estimate of $A_V = 2.16$, substantially more than for CM Cyg. Figure 3 plots the dereddened photometry.

Figure 3 also presents some estimates of possible continua in the spectrum of CSS 1005. The *K*-band amplitude is about as large as observed for a Mira variable (see, e.g., Whitelock et al. 2000). We have chosen the intermediate brightness as observed on JD 2454232 (2007 May 11) to split the possible errors. Molecular absorption should affect *K* and *L* less than the shorter-wavelength filters. Forcing a Planck function through these requires a temperature of 3000 K. The resulting continuum comes close to the IRS data. If we assume that iron dust (with $a = 0.3 \mu\text{m}$) accounts for the difference and that the spectrum at $7.5\text{--}9.5 \mu\text{m}$ is the “continuum,” then an excess of 34% is

required at $10 \mu\text{m}$ and the dust is at $\sim 270 \text{ K}$.¹³ As before, we can also force the continuum through the peaks in the spectrum, which requires a grain temperature of 300 K and an excess of 65% at $10 \mu\text{m}$. Amorphous carbon grains of $0.1 \mu\text{m}$ radius at a temperature of 230 K would fit the lower continuum with a 35% excess. The upper continuum requires a temperature of 280 K and an excess of 63%.

Thus, CSS 1005 presents us with the same uncertainties as CM Cyg. And for the same reasons, we will proceed with the fit to the underside of the IRS spectrum. With this interpretation, CSS 1005 shows apparent emission features at 7, 11, and $13\text{--}14 \mu\text{m}$, like CM Cyg, and it shows an additional emission feature at $21 \mu\text{m}$ as well.¹⁴

The pulsation period of CSS 1005 is unknown, preventing us from estimating its distance. Estimates of the dust mass required for the excesses in Figure 3 depend sensitively on distance (d^2). Given that the discussion in Section 3.1 for CM Cyg is already fraught with assumptions, we will defer discussion of the location and mass of the dust in the outflows of CSS 1005 until more is known about the central star.

3.3. Amorphous Alumina

Figure 4 presents the spectra of CM Cyg and CSS 1005 after removing the iron dust pseudo-continua in Figures 2 and 3 fitted through the spectra at $7.5\text{--}9.5 \mu\text{m}$. If the remaining excess is truly emission, then the dominant component, in terms of integrated flux, is amorphous alumina.

To illustrate this fact, we turn to the spectrum of another S star in Program 30737, CSS 1, in Figure 5. This source has an unusually strong alumina excess, which we can fit using the optical constants for porous alumina grains measured by Begemann et al. (1997). Their data extend from $7.8 \mu\text{m}$ to the red, and we have supplemented them by splicing the measurements by Koike et al. (1995) at shorter wavelengths. The laboratory sample fits the spectrum of CSS 1 well at a dust temperature of 600 K. The observed spectrum and the laboratory opacities differ below $10 \mu\text{m}$, but with our simplistic assumptions about the stellar continuum, these differences may not be significant.

To remove the contribution of alumina from the residual spectra of CM Cyg and CSS 1005 in Figure 4, we set the dust-grain temperature to 1600 K and fitted the emission to the spectra at $11.5\text{--}12 \mu\text{m}$. While the higher dust temperature compared to CSS 1 is consistent with the lower dust opacities in CM Cyg and CSS 1005, the detailed shape of the alumina feature depends on our assumed continuum and should be considered tentative at this stage.

The porous alumina of Begemann et al. (1997) provides the best fit available to these two spectra and to CSS 1, better than their compact grains, which are too transparent to the red, and better than the samples studied by Koike et al. (1995), which have emission features which peak closer to $12 \mu\text{m}$. But there are some discrepancies between the porous alumina and the observed spectra. Both spectra suggest that the laboratory constants are too opaque below $10 \mu\text{m}$, and in CM Cyg, too opaque at $\sim 17 \mu\text{m}$ as well. It remains to be seen if these differences survive more careful modeling of the continuum.

¹³ This dust temperature is cooler than for CM Cyg, but it is sensitive to the assumed continuum, and the difference may not be significant.

¹⁴ This feature brings to mind the “ $21 \mu\text{m}$ ” feature detected in carbon-rich post-AGB objects; that feature is actually centered at $20 \mu\text{m}$, and it is associated with other carbon-rich dust features not seen in these spectra.

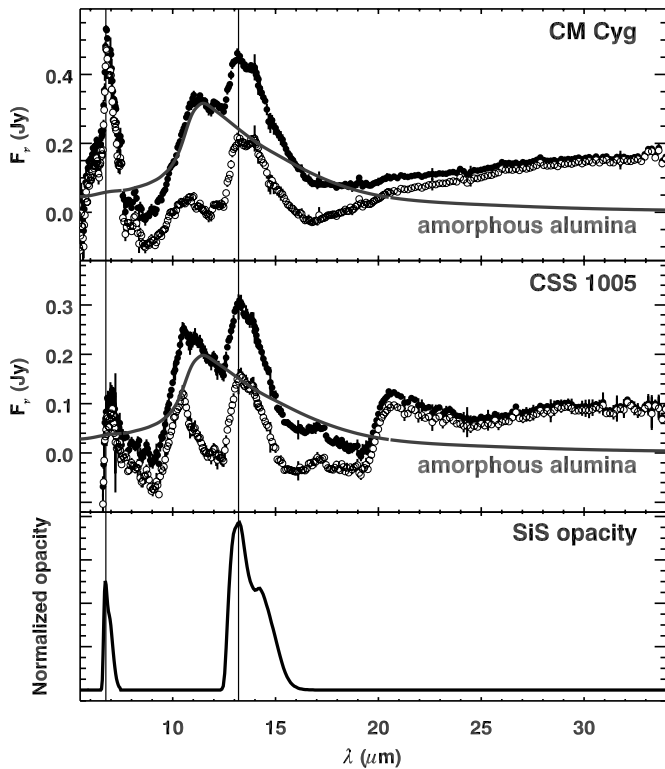


Figure 4. Top two panels show the spectra of CM Cyg and CSS 1005 after subtracting the pseudo-continua depicted by the dashed lines in Figures 2 and 3 (filled circles). Removing amorphous alumina grains with a temperature of 1600 K leaves a residual (open circles) with strong features at 6.75 and 13–14 μm , which we identify as emission from SiS molecules. The comparison spectrum in the bottom panel is SiS as fitted to the spectrum of CSS 100 by Cami et al. (2009).

In the spectrum of CSS 1005, the alumina feature peaks closer to 10 μm , leaving a more substantial residual after removing the contribution from alumina. We have been unable to correct this by adding silicates of any kind. The emission feature from amorphous silicates is too broad, and no crystalline species will produce just this single narrow 10 μm feature. We do not know its origin.

3.4. Molecular SiS Emission

In Figure 4, the difference spectra of both objects show a narrow emission feature near 7 μm and a broader feature with a peak at 13 μm and a shoulder at 14 μm . Given that the dust emission from these sources is clearly alumina-rich, it is tempting to identify the carrier of the 13 μm feature as an Al–O stretching mode in dust grains, either from crystalline alumina (Al_2O_3 ; Glaccum 1995; Sloan et al. 1996) or spinel (MgAl_2O_4 ; Posch et al. 1999; Fabian et al. 2001). Neither spectrum shows a 32 μm feature expected of spinel, although CSS 1005 does have a weak feature near 16.8 μm , where spinel should show a secondary feature. Interestingly, CSS 1005 has a noticeable emission feature at 21 μm and a weaker one at 28 μm . The former corresponds to the position of a weak feature observed from crystalline alumina by Toon et al. (1976). The latter could be the 28 μm feature observed in oxygen-rich dust shells. In that case, its strength is correlated with that of the 13 μm dust feature (Sloan et al. 2003). But we may also be seeing a 26–30 μm feature attributed to MgS (Goebel & Moseley 1985). Thus in CM Cyg, a contribution at 13 μm from aluminum-rich dust is unlikely, but in CSS 1005, some contribution may be possible.

SiS is also known to produce spectroscopic features at 13 μm . Morris et al. (1975) discovered emission from SiS at millimeter wavelengths in the extensive envelope around the carbon star IRC +10216 (see also Sahai et al. 1984). Boyle et al. (1994) identified absorption bands from 13.0 to 13.4 μm from the fundamental stretching mode of SiS in the infrared spectrum of the same object. Aoki et al. (1998) identified overtone absorption bands of SiS between 6.6 and 6.8 μm in the spectrum of WZ Cas obtained with the Short-Wavelength Spectrometer aboard the *Infrared Space Observatory*. WZ Cas is an SC star like CM Cyg and thus has a C/O ratio very close to 1.00. Aoki et al. expected the strongest SiS abundances at precisely this C/O ratio, because SiO will exhaust the available silicon at lower C/O ratios, and CS will exhaust the sulfur at higher C/O ratios.

The IRS spectra cannot resolve the detailed band structure, but the observed features are at the positions expected for SiS. Furthermore, Cami et al. (2009) have recently identified both bands in absorption in several other S stars in Program 30737. The fundamental absorption band is readily identifiable in 18 of the 90 spectra in the sample, which is over one-third of the 53 naked stars observed.

Figure 4 includes a comparison SiS spectrum, based on the model fitted by Cami et al. (2009) to CSS 100 (see their Figure 2) for gas at a temperature of 2900 K. We have inverted the absorption to make the comparison easier. The overtone mode is centered at 6.75 μm , which closely matches the sharp emission feature in the spectrum of CM Cyg. In CSS 1005, the feature is noisier and broader, but it is still close to the correct position. The comparison model accurately reproduces the general shape of the emission at 13–14 μm as well, with a peak at 13 μm and a shoulder at 14. Our identification is based primarily on the wavelengths of the two bands. The relative strengths vary significantly among the sample presented by Cami et al. (2009), and for our sources, are strongly dependent on the nature of the assumed continuum, especially in the vicinity of 7 μm .

4. DISCUSSION

While we cannot definitively identify the continuum in our IRS spectra, pinning it to the valleys in the spectrum results in a mixture of dust and gas emission which is fully consistent with the unusual chemistry in the outflows from S stars. When oxygen only slightly outnumbered carbon, the formation of CO will leave very little oxygen to form dust or its precursors. Sloan & Price (1998) suggested that this mechanism explained the observed lack of silicate grains in dust shells around S stars. Alumina condenses before silicates, due to the higher condensation temperature, and more importantly to the higher chemical affinity of oxygen for aluminum compared to silicon (Stencel et al. 1990). The chemical affinity would explain the absence of SiO bands in the two spectra here. And of course, the appearance of sulfides such as SiS is a natural consequence of the lack of available oxygen. The presence of SiO bands in some of the naked stars with SiS absorption bands in the larger S-star sample may indicate that the C/O ratios in those objects are typically lower than in CM Cyg and CSS 1005.

Both iron grains and amorphous carbon dust could explain the difference between the apparent continuum and the photostellar continuum inferred from photometry at shorter wavelengths in the spectra of CM Cyg and CSS 1005. Consideration of the dust mass required and the chemistry of the outflows makes iron the more likely candidate. McDonald et al. (2010) proposed iron dust based on IRS spectra of metal-poor oxygen-rich AGB stars in globular clusters, after considering several alternatives. The

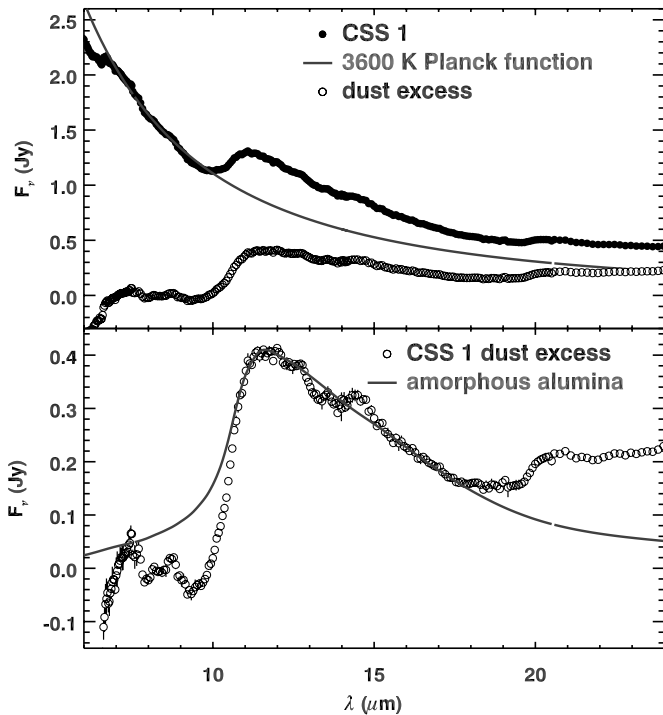


Figure 5. Amorphous alumina dust in the spectrum of the S star CSS 1. In the top panel, the dust excess is isolated by fitting and removing a 3600 K Planck function. The bottom panel shows that the residual is fitted well with the porous alumina sample measured by Begemann et al. (1997). The grains have an assumed temperature of 600 K.

key to the detection appears to be the relative lack of other dust species, due in that case to the low metallicity of the stars. In the S stars, the absence of silicate emission arises from the unusual chemistry. In either case, examining the spectra from mass-losing stars with weak silicate features makes it possible to observe other condensates which would ordinarily be buried spectroscopically by the silicate emission.

BFM 1, an S star in the SMC, also shows a 13–14 μm emission feature (Sloan et al. 2008). Two IRS spectra of this source were obtained 418 days apart (compared to the star’s 398 day pulsation period), and the 13–14 μm emission feature appears in only the first spectrum. Despite this spectral variability, the presence of this feature in two S stars in the Galaxy and one in the SMC and in no objects with different chemistries gives us confidence that the detection in BFM 1 is real and related to the features in CM Cyg and CSS 1005.

The primary objective of this paper is to identify the carrier of the 13–14 μm feature. The identification of SiS relies on a match to two bands, including the narrower one at 7 μm , and we believe it to be reasonably secure, despite the uncertainties on how to fit the continuum. Higher-resolution spectroscopy which should reveal the molecular band structure would provide confirmation. This identification is important because of a natural tendency to assume that broad emission features such as these arise from dust grains.

In BFM 1, the SiS emission has dissipated in a short time. The transitory nature of the SiS emission suggests a stochastic emission process for these bands, leaving open the question of what we would see if we were able to re-observe BFM 1, CM Cyg, CSS 1005, or the other 18 stars in the S-star sample with SiS absorption in their spectra. A more detailed analysis of the SiS bands observed in both emission and absorption is forthcoming. In the meantime, we can speculate that the emission bands could

arise from shocked gas. All three objects with SiS emission are Mira variables, which are commonly associated with shocked emission. Additional sources in the S-star sample show weaker emission features which may also arise from SiS, and they too are Mira variables. Other possible causes include fluctuations in the mass-loss rate or photospheric chemistry. Assumptions of a spherically symmetric emission region might be unwise in these cases.

In addition to the featureless excess and SiS bands, the spectra of CM Cyg and CSS 1005 show other interesting emission features. Both have an excess to longer wavelengths, which probably arises from a population of cooler grains further away from the stars and ejected in earlier mass-loss episodes.

The 21 μm feature in the spectrum of CSS 1005 is particularly intriguing. One of the difficulties with the identification of crystalline alumina as the carrier of the 13 μm feature is that a 21 μm feature should also be present. The only way to avoid this problem is to invoke hot dust grains, which is consistent with the higher condensation temperature of alumina. It is possible that the 21 μm feature in the spectrum of CSS 1005 indicates a population of cool crystalline alumina grains, and that a warmer population might be contributing to the feature we have identified as due to SiS. While that might explain the difference in contrast of the 7 μm SiS feature to the 13 μm feature, one should keep in mind that the uncertainty in the continuum fitting contributes to the uncertainty in the 7/13 μm strength ratio. Another difficulty to consider is the presence of the 21 μm feature in the spectrum of CSS 1. In this case, no 13 μm feature is obvious, and if crystalline alumina were responsible for the 21 μm feature, the grains would have to be quite cold to suppress the stronger feature at 13 μm .

The spectrum of CSS 1005 presents another challenge: the nature of the excess emission centered at 10.5 μm . Perhaps this is a crystalline grain component of some kind, but if it were a silicate, one would expect more spectral structure between 9 and 10 μm . It may be another molecule, or perhaps some modification to the amorphous alumina structure.

To conclude, the spectra of CM Cyg and CSS 1005 are rich with clues about the formation of molecules and the condensation of dust in the outflows of stars where the abundances of carbon and oxygen are nearly equal. Some of these clues strongly reinforce our expectations in these cases, but others remain enigmatic. While these objects may be highly unusual, they give us insight into a process common to nearly all stars as they evolve past their main-sequence lifetimes.

We thank the anonymous referee, whose comments and questions helped us improve this paper. We are also grateful to I. McDonald and D. Chernoff for their valuable input concerning the contribution of dust to these spectra. The observations were made with the *Spitzer Space Telescope*, which is operated by JPL, California Institute of Technology under NASA contract 1407 and supported by NASA through JPL (contract no. 1257184). This research used the AAVSO International Database and the SIMBAD and VIZIER databases, operated at the Centre de Données astronomiques de Strasbourg.

REFERENCES

- Ake, T. B. 1979, *ApJ*, 234, 538
 Aoki, W., Tsuji, T., & Ohnaka, K. 1998, *A&A*, 340, 222
 Begemann, B., Dorschner, J., Henning, Th., Mutschke, H., Guertler, J., Koempe, C., & Nass, R. 1997, *ApJ*, 476, 199

- Beichman, C. A., Neugebauer, G., Habing, H. J., Clegg, P. E., & Chester, T. J. 1988, *Infrared Astronomical Satellite (IRAS) Catalogs and Atlases*, Vol. 1 Explanatory Supplement (Pasadena, CA: JPL)
- Bidelman, W. P. 1950, *ApJ*, **112**, 219
- Boyer, M. L., et al. 2009, *ApJ*, **705**, 746
- Boyle, R. J., Keady, J. J., Jennings, D. E., Hirsch, K. L., & Wiedemann, G. R. 1994, *ApJ*, **420**, 863
- Cami, J., Sloan, G. C., Markwick-Kemper, A. J., Zijlstra, A. A., Bauschlicher, C. W., Matsuura, M., Decin, L., & Hony, S. 2009, *ApJ*, **690**, L122
- Catchpole, R. M., Robertson, B. S. C., Lloyd Evans, T. H. H., Feast, M. W., Glass, I. S., & Carter, B. S. 1979, *Circ. South Afr. Astron. Obs.*, **1**, 61
- Engelke, C. W. 1992, *AJ*, **104**, 1248
- Engelke, C. W., Price, S. D., & Kraemer, K. E. 2006, *AJ*, **132**, 1445
- Fabian, D., Posch, Th., Mutschke, H., Kerschbaum, F., & Dorschner, J. 2001, *A&A*, **373**, 1125
- Fujita, Y. 1939, *Japan. J. Astron. Geophys.*, **17**, 17
- Fujita, Y. 1940, *Japan. J. Astron. Geophys.*, **18**, 45
- Glaccum, W. 1995, in *ASP Conf. Ser. 73, The Airborne Astronomy Symposium on the Galactic Ecosystem*, ed. M. R. Haas, J. A. Davidson, & E. F. Erickson (San Francisco, CA: ASP), 395
- Goebel, J. H., & Moseley, S. H. 1985, *ApJ*, **290**, L35
- Habing, H. J. 1996, *A&AR*, **7**, 97
- Houck, J. R., et al. 2004, *ApJS*, **154**, 18
- Iben, I., Jr., & Renzini, A. 1983, *ARA&A*, **21**, 271
- Ishihara, D., et al. 2010, *A&A*, **514**, A1
- Keenan, P. C. 1948, *ApJ*, **107**, 420
- Keenan, P. C. 1966, in *IAU Symp. 24, Spectral Classification and Multicolour Photometry*, ed. K. Lodén, L. O. Lodén, & U. Sinnerstand (London: Academic), 26
- Keenan, P. C., & Boeshaar, P. C. 1980, *ApJS*, **43**, 379
- Koike, C., Kaito, C., Yamamoto, T., Shibai, H., Kimura, S., & Suto, H. 1995, *Icarus*, **114**, 203
- Kraemer, K. E., Sloan, G. C., Price, S. D., & Walker, H. J. 2002, *ApJS*, **140**, 389
- McDonald, I., Sloan, G. C., Zijlstra, A. A., Matsuura, N., Matsuura, M., Kraemer, K. E., Bernard-Salas, J., & Markwick, A. J. 2010, *ApJ*, **717**, L92
- McDonald, I., van Loon, J. T., Decin, L., Boyer, M. L., Dupree, A. K., Evans, A., Gehrz, R. D., & Woodward, C. E. 2009, *MNRAS*, **394**, 831
- Merrill, P. W. 1922, *ApJ*, **56**, 457
- Merrill, P. W. 1923, *PASP*, **35**, 217
- Morris, M., Gilmore, W., Palmer, P., Turner, B. E., & Zuckerman, B. 1975, *ApJ*, **199**, L47
- Moshir, M., et al. 1990, *IRAS Faint Source Catalogue*, version 2.0
- Neguereuela, I., & Marco, A. 2008, *A&A*, **492**, 441
- Ordal, M. A., Bell, R. J., Alexander, R. W., Jr., Newquist, L. A., & Querry, M. R. 1988, *Appl. Opt.*, **27**, 1203
- Posch, T., Kerschbaum, F., Mutschke, H., Fabian, D., Dorschner, J., & Hron, J. 1999, *A&A*, **352**, 609
- Rieke, G. H., & Lebofsky, M. J. 1985, *ApJ*, **288**, 618
- Sahai, R., Wootten, A., & Clegg, R. E. S. 1984, *ApJ*, **284**, 144
- Schlegel, D. J., Finkbeiner, D. P., & Davis, M. 1998, *ApJ*, **500**, 525
- Skrutskie, M. F., et al. 2006, *AJ*, **131**, 1163
- Sloan, G. C., Kraemer, K. E., Goebel, J. H., & Price, S. D. 2003, *ApJ*, **594**, 483
- Sloan, G. C., Kraemer, K. E., Wood, P. R., Zijlstra, A. A., Bernard-Salas, J., Devost, D., & Houck, J. R. 2008, *ApJ*, **686**, 1056
- Sloan, G. C., Levan, P. D., & Little-Marenin, I. R. 1996, *ApJ*, **463**, 310
- Sloan, G. C., & Price, S. D. 1998, *ApJS*, **119**, 141
- Smith, B. J., Price, S. D., & Moffett, A. J. 2006, *AJ*, **131**, 612
- Stencel, R. E., Nuth, J. A., III, Little-Marenin, I. R., & Little, S. J. 1990, *ApJ*, **350**, L45
- Stephenson, C. B. 1984, *Publ. Warner Swasey Obs.*, **3**, 1
- Templeton, M. R., Mattei, J. A., & Willson, L. A. 2005, *AJ*, **130**, 776
- Toon, O. B., Pollack, J. B., & Khare, B. N. 1976, *J. Geophys. Res.*, **81**, 5733
- Werner, M. W., et al. 2004, *ApJS*, **154**, 1
- Whitelock, P. A., Feast, M. W., & van Leeuwen, F. 2008, *MNRAS*, **386**, 313
- Whitelock, P. A., Marang, F., & Feast, M. 2000, *MNRAS*, **319**, 728
- Yang, X., Chen, P., Wang, J., & He, J. 2006, *AJ*, **132**, 1468
- Zubko, V. G., Mennella, V., Colangeli, L., & Bussoletti, E. 1996, *MNRAS*, **282**, 1321